6th European Conference on Computational Mechanics (ECCM 6)
7th European Conference on Computational Fluid Dynamics (ECFD 7)
1115 June 2018, Glasgow, UK

ISOGEOMETRIC ANALYSIS IN FLUID-STRUCTURE INTERACTION PROBLEMS CONSIDERING STRUCTURAL CONTACT

Daniel Hilger[1], **Norbert Hosters**[1], **Marek Behr**[1], **Stefanie Elgeti**[1]

[1]Chair for Computational Analysis of Technical Systems (CATS), RWTH Aachen University,
Schinkelstrasse 2, 52062 Aachen, Germany,
e-mail: {hilger, hosters, behr, elgeti}@cats.rwth-aachen.de, www.cats.rwth-aachen.de

Key words: Isogeometric Analysis (IGA), NURBS, fluid-structure interaction (FSI), computational contact mechanics, NURBS

Abstract. Fluid-structure interactions (FSI) problems considering contact are complex dynamical processes that, when numerically analyzed, require special treatment especially of the coupling between the fluid and the structure. In the context of this paper, the governing equations and numerical methods used to describe a full FSI problem are briefly recapitulated. Based on the test case of a structural ring falling inside a fluid tank, the implementation of isogeometric analysis (IGA) on the structural side combined with a non-uniform rational B-splines (NURBS-) based method on the fluid side is presented for FSI problems that include contact. As part of the test case, the influence of the interface representation on the detection of contact zones and the coupling in FSI is investigated.

1 INTRODUCTION

This paper is on the subject of fluid-structure interactions; or, more specifically, FSI phenomena that include structural contact. These occur, for example, in valves, pumps, or pistons. FSI problems belong to the category of multiphysics problems, for the solution of which three different strategies can be pursued: (1) field elimination, (2) a monolithic approach, or (3) a partitioned approach [5].

In this paper, we apply the partitioned solution strategy, where all involved field problems are solved individually, yet are coupled via connected boundary conditions at their common interface. To ensure consistent coupling, the involved problems must be coupled in both space and time [14]. For the temporal coupling, either a weak or a strong coupling approach can be applied. In the strong coupling approach used within this work, the different field problems are solved iteratively until the current solution converges to an equilibrium state [14]. In case of non-matching discretizations at the fluid-structure interface, additional spatial coupling is required for consistent transformation of displacements and loads. This is for example achieved by coupling schemes such as the finite interpolation method [4]. In the special case of NURBS-enhanced finite elements (NEFEM) on the fluid side and IGA on the structural side, an identical representation of the interface exists, allowing a direct integration of the fluid forces on the interface [6].

In context of this work an IGA approach is pursued for the structural analysis for two reasons: (1) it provides a smooth surface representation of the FSI interface, and (2) the parametric description of the surface offers advantages in the detection of the contact areas [11]. In IGA, splines – such as non-uniform rational B-splines (NURBS)– are used to provide both a parametric representation of the geometry [10] and an approximation of the solution space [2].

In FSI, the displacement of the structure always involves the change in the fluid domain. In principle, this deformation can be traced either by an interface capturing or by an interface tracking[3]. In this work, we focus on boundary conforming meshes and an interface tracking approach. This leads to a deformation of the fluid mesh according to the interface motion. Solving the fluid problem with the deforming-spatial-domain/stabilized space-time (DSD/SST) method [12, 13] enables a calculation of the mesh deformation independently of the fluid problem. Thus, additional mesh deformation methods, such as the elastic mesh update method (EMUM), can be utilized to adapt the computational mesh to the deformed domain [9].

This paper is structured as follows. Section 2 introduces the governing equations and numerical methods used within this work. In section 3 a numerical test case is presented, showing the application of IGA in a FSI problem considering structural contact.

2 GOVERNING EQUATIONS AND NUMERICAL METHODS

Following the partitioned solution approach, the FSI problem is decomposed into three individual field problems for (1) the structural deformation, (2) the fluid flow, and (3) the deformations of the computational mesh. Each field problem is described individually by a set of equations that are connected via boundary conditions at the fluid-structure interface. These boundary conditions are defined through the kinematic and dynamic coupling conditions of FSI.

2.1 Structural deformation considering contact interaction

Consider the structural object as a bounded domain Ω_t^s in R^{nsd}, where nsd indicates the number of spatial dimensions. For every time $t \in [0, T]$ the displacement $\mathbf{d}\,(\mathbf{x}, t)$ for every point $\mathbf{x} \in \Omega_t^s$ can be expressed by the equation of motion, defined on the reference configuration Ω_0^s:

$$\rho^s \frac{\partial^2 \mathbf{d}^s}{\partial t^2} = \boldsymbol{\nabla}_0 \cdot \mathbf{S}^s \mathbf{F}^T + \rho_0^s \mathbf{b}^s \qquad \text{in } \Omega_0^s \times [0, T]\,, \tag{1}$$

where ρ^s indicates the density of the structure, $\mathbf{S}^s$ represents the 2nd Piola-Kirchhoff stress tensor, $\mathbf{F}$ the deformation gradient, and $\mathbf{b}^s$ denotes the body force per unit volume. The constitutive equation for the stress tensor is, in our case, provided by the St. Venant-Kirchhoff model, stating a linear stress-strain relation between the 2nd Piola-Kirchhoff stress tensor and on the Green-Lagrange strain tensor $\mathbf{E}^s$. With the Lamé constants λ^s and μ^s the stress tensor is defined as follows,

$$\mathbf{S}^s\left(\mathbf{E}\right) \;=\; \lambda^s \mathrm{tr}\left(\mathbf{E}^s\right) \,+\, 2\mu^s \mathbf{E}^s, \tag{2}$$

with

$$\mathbf{E}^s \;=\; \frac{1}{2}\left(\mathbf{F}^T\mathbf{F} \,-\, \mathbf{I}\right) \tag{3}$$

and

$$\mathbf{F} \;=\; \frac{\partial \mathbf{x}}{\partial \mathbf{x}_0}. \tag{4}$$

Dirichlet and Neumann boundary conditions are applied to the boundary that can be split into two complementary parts, i.e. $\Gamma^s_t \;=\; \Gamma^s_{t,g} \cup \Gamma^s_{t,h}$.

$$\mathbf{d}^s = \mathbf{g}_s \quad \text{on } \Gamma^s_{t,g} \times [0,T]\,, \tag{5a}$$

$$\boldsymbol{\sigma}^s \cdot \mathbf{n} = \mathbf{h}^s \quad \text{on } \Gamma^s_{t,h} \times [0,T]\,. \tag{5b}$$

In this paper, the contact interaction of the structural object is restricted to interaction with a stiff, rigid obstacle. For the area of contact, additional pressure contributions p_N act on the structural object. These areas are determined by the normal distance g_n, which is defined as distance between predefined positions $\mathbf{x}^s_c$, distributed on the surface of structural object Γ^s, and their associated closest-point projections $\mathbf{x}_{cpp}$ on the obstacle surface,

$$g_N \;=\; \left(\mathbf{x}_{cpp} \,-\, \mathbf{x}^s_c\right) \cdot \mathbf{n}_s. \tag{6}$$

Due to the no-penetration condition, discussed in detail in [15], the structural contact interactions can be formulated as constraints on the equilibrium equation in (1). These constraints are called Hertz-Signorini-Moreau constraints and defined as follows:

$$g_N \geq 0\,, \qquad p_N \leq 0\,, \qquad p_N g_N \;=\; 0. \tag{7}$$

2.1.1 Isogeometric analysis

In IGA, the isoparametric concept is applied by using NURBS basis functions for both geometry representation and approximation of the solution [2]. This allows an exact initial representation of the geometry. IGA is discussed in detail in [7, 2]. The representation of NURBS objects is based on a linear combination of NURBS basis functions $R_{i,p}$, with polynominal degree p, and control points $\mathbf{P}_i$ [10],

$$\mathbf{C}\left(\boldsymbol{\xi}\right) \;=\; \sum_{i=1}^{ncp} R_{i,p}\,\mathbf{P}_i. \tag{8}$$

Especially important properties of NURBS in the context of FSI and contact interaction is the almost arbitrarily control of the continuity of the geometry and interface representation [11, 6].

2.1.2 Penalty method

Within this work the compliance of the structural solution with the Hertz-Signorini-Moreau constraints is ensured via the penalty method. A detailed description of the implementation of the penalty method in contact mechanics is described in [15]. However, the basic concept pursued in the penalty method is that violations of the constraints are punished by an additional contribution to the equilibrium equation.

2.2 Governing equations for fluid flow

The fluid problem is solved on the computational domain $\Omega_t^f \subset \mathrm{R}^{nsd}$. In incompressible fluid flows we solve for the unknown fields of velocity $\mathbf{u}(\mathbf{x}, t)$ and pressure $p(\mathbf{x}, t)$. For every time $t \in [0, T]$, the fluid's behavior is governed by the Navier-Stokes equations for incompressible fluids:

$$\rho^f \left(\frac{\partial \mathbf{u}^f}{\partial t} + \mathbf{u}^f \cdot \boldsymbol{\nabla} \mathbf{u}^f - \mathbf{f}^f \right) - \boldsymbol{\nabla} \cdot \boldsymbol{\sigma}^f = \mathbf{0} \qquad \text{on } \Omega_t^f, \forall t \in [0, T], \tag{9a}$$

$$\boldsymbol{\nabla} \cdot \mathbf{u}^f = \mathbf{0} \qquad \text{on } \Omega_t^f, \forall t \in [0, T], \tag{9b}$$

with ρ^f denoting the fluid density and $\mathbf{f}^f$ representing all external body forces. For Newtonian fluids, the stress tensor σ^f is defined as

$$\boldsymbol{\sigma}^f = -p^f \mathbf{I} + 2\rho^f \nu^f \boldsymbol{\varepsilon}^f \left(\mathbf{u}^f\right), \tag{10}$$

with

$$\boldsymbol{\varepsilon}^f \left(\mathbf{u}^f\right) = \frac{1}{2} \left(\boldsymbol{\nabla} \mathbf{u}^f + \left(\boldsymbol{\nabla} \mathbf{u}^f\right)^T \right), \tag{11}$$

where ν^f denotes the dynamic viscosity. A well-posed system is obtained, when boundary conditions are imposed on the external boundary Γ^f. Here, we distinguish between Dirichlet and Neumann boundary conditions given by:

$$\mathbf{u}^f = \mathbf{g}^f \text{on } \Gamma_g^f, \tag{12a}$$

$$\mathbf{n}^f \cdot \boldsymbol{\sigma}^f = \mathbf{h}^f \text{on } \Gamma_h^f, \tag{12b}$$

where $\mathbf{g}^f$ and $\mathbf{h}^f$ prescribe the velocity and stress values on complementary subsets of Γ^f.

The Navier-Stokes equation in (9) are solved by the DSD/SST method discussed in detail in [12, 13]. Here, space and time are discretized by the finite element approach, implicitly including the domain deformation into the solution method. Thus, the mesh deformation can be computed detached from the solution of the Navier-Stokes equations [12]. Further, the space-time formulation is stabilized by the Galerkin/Least-Squares (GLS) and the streamline upwind/Petrov-Galerkin (SUPG) stabilization [1], to avoid oscillations in the solutions of pressure and velocity.

2.3 Coupling conditions at fluid-structure interface

The fluid and the structural problem are connected via their common interface $\Gamma_{FS} = \Gamma^f \cup \Gamma^s$. For a consistent coupling of the structural and the fluid problem, the coupling conditions need to fulfill the kinematic continuity, ensuring the displacements and velocity across the interface,

$$\mathbf{d}^f = \mathbf{d}^s \qquad \text{on } \Gamma_{FS}, \tag{13a}$$

$$\mathbf{u}^f = \mathbf{u}^s \qquad \text{on } \Gamma_{FS}, \tag{13b}$$

and the dynamic continuity, enforcing the continuity of fluid and structural stresses at the interface,

$$\boldsymbol{\sigma}^f \cdot n^f = -\boldsymbol{\sigma}^s \cdot n^s \qquad \text{on } \Gamma_{FS}. \tag{14}$$

2.4 Elastic mesh update-method

The boundaries of the fluid domain Γ_f deform according to the displacements of the structural object. Thus, the computational mesh has to be deformed according to boundary movements. A method utilized for the automatic mesh update is the elastic mesh update method (EMUM), first presented in [9]. The mesh is considered an elastic body, where the displacements of the internal nodes are governed by the equilibrium equations of elasticity:

$$\boldsymbol{\nabla} \cdot \boldsymbol{\sigma}^{Mesh} = \mathbf{0}. \tag{15}$$

$$\tag{16}$$

Therin, the stress tensor σ^{Mesh} is related to the strain tensor ε^{Mesh} via

$$\boldsymbol{\sigma}^{Mesh} = \lambda^{Mesh} \left(\mathrm{tr}\boldsymbol{\varepsilon}^{Mesh}(\mathbf{d})\right) \mathbf{I} + 2\mu\boldsymbol{\varepsilon}^{Mesh}(\mathbf{d}), \tag{17a}$$

$$\boldsymbol{\varepsilon}^{Mesh}(\mathbf{d}) = \frac{1}{2}\left(\boldsymbol{\nabla}\mathbf{d} + (\boldsymbol{\nabla}\mathbf{d})^T\right). \tag{17b}$$

with the Lamé constants λ^{Mesh} and μ^{Mesh}. In the context of FSI, the employed Dirichlet boundary conditions correspond to the displacement of the fluid-structure interface

$$\mathbf{d}^{Mesh} = \mathbf{d}^s \qquad \text{on } \Gamma_{FS}. \tag{18}$$

The EMUM used within this paper is extended by a method, allowing large translations of the structural object within the fluid domain, following the concept in [8].

3 TEST CASE

In this test case we demonstrate the application of IGA and NURBS-based methods in the context of a FSI problem that includes structural contact. In particular, we examine the influence of the interface representation on the solution. For that purpose we observe a structural ring, falling inside a fluid filled tank.

The fluid domain has a height and width of 1.0 m. At a height of 0.75 m, the ring is centrally positioned in the fluid domain. The ring has a diameter of 0.08 m and a thickness of 0.015 m. Material properties of fluid and structure are chosen according to Table 1. The ring is accelerated by a gravitational body force and thus causes a fluid flow around the moving ring. Initially, the fluid and the ring are in rest. Figures 2 to 6 show the flow field inside the tank for five exemplary points in time.

parameter	value
dynamics viscosity	$1.82 \cdot 10^{-5}$ kg/ms
density (fluid)	1.2041 kg/m^3
Young's Modulus	$6.9 \cdot 10^9$
Poisson number	0.34
density (structure)	2730 kg/m^3

Table 1: Material parameters of FSI components

In the following the solutions of the FSI problem is compared for two discretization strategies of the fluid-structure interface Γ_{FS}. First, an approach with NURBS based interface representation of both sides of the interface – namely NEFEM on the fluid side and IGA on the structural side – is used, and second an approach using a NURBS representation of the structure interface, yet standard finite elements (SFEM) for the representation of the fluid interface. In the second approach, the finite interpolation method is used additionally to exchange boundary conditions at the FSI interface.

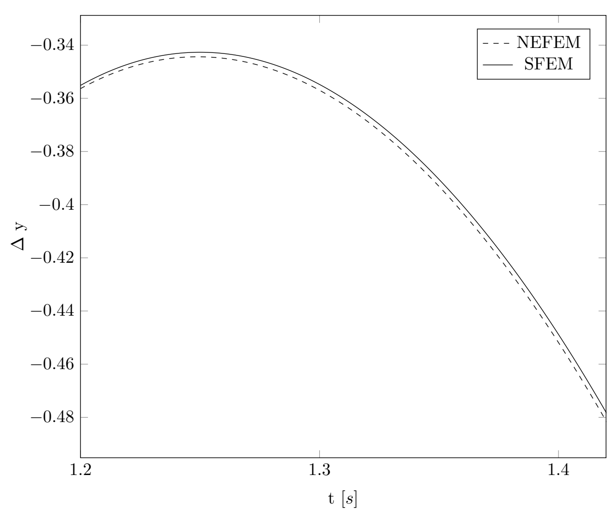

Figure 1: y-displacement of ring in FSI problem

In Figure 1 we present an excerpt of the graph, displaying the displacement of the ring. A difference between the two computed solutions is clearly noticeable. This discrepancy must result directly from the different interface representation, since all other discretizations of the problem coincide.

4 CONCLUSIONS

In context of this paper, we presented a test case for FSI including structural contact. Therein, the influence of interface representations were examined. It could be shown that solely by the use of coinciding boundary representation an improvement in accuracy of the solution could be achieved. This affirms the use of NURBS based methods for all problems including moving interfaces.

ACKNOWLEDGMENT

This work was supported by the German Research Foundation unter the Cluster of Excellence "Integrative production technology for high-wage countries". Computing resources were provided by the AICES graduate school and RWTH Aachen University Center for Computing.

REFERENCES

[1] Behr, M. *Stabilized Finite Element Method for Incompressible Flows with Emphasis on Moving Boundaries and Interfaces.* PhD thesis, University of Minnesota, (1992).

[2] J.A. Cottrell, T.J.R. Hughes, and Y. Bazileves. *Isogeometric analysis: toward integration of CAD and FEA* John Wiley & Sons, (2009).

[3] S. Elgeti, and H. Sauerland. *Deforming fluid domains within the finite element method: five mesh-based tracking methods in comparison*. Archives of Computational Methods in Engineering, (2016), Vol. 23, pp 323–361.

[4] C. Farhat, M. Lesoinne, and P. Le Tallec. *Load and motion transfer algorithms for fluid/structure interaction problems with non-matching discrete interfaces: Momentum and energy conservation, optimal discretization and application to aeroelasticity.* Computer methods in applied mechanics and engineering, (1998), Vol 157. , pp 95–114 .

[5] C.A. Felippa, K.C. Park, and C. Farhat. *Partitioned analysis of coupled mechanical systems*. Computer methods in applied mechanics and engineering, (2001), Vol. 190, pp 3247–3270.

[6] N. Hosters, J. Helmig, A. Stavrev, M. Behr, and S. Elgeti *Fluid-Structure Interaction with NURBS-Based Coupling.* Accepted to Computer Methods in Applied Mechanics and Engineering, (2017).

[7] T.J.R. Hughes, J.A. Cottrell, and Y. Bazileves. *Isogeometric analysis:CAD, finite elements, NURBS, exact geometry and mesh refinement.* Computer methods in applied mechanics and engineering, (2005), Vol. 194, pp 4135–4195.

[8] F. Key, L. Pauli, and S. Elgeti. *The Virtual Ring Shear-Slip Mesh Update Method.* submitted to Computer and Fluids, (2018).

[9] A.A. Johnson, and T.E. Tezduyar. *Mesh update strategies in parallel finite element computations of flow problems with moving boundaries and interfaces.* Computational Methods in Applied Mechanical Engineering, (1994), Vol. 119 (1994):73–94.

[10] L. Piegel, and w. Tiller. *The NURBS book.* Springer, Berlin, (1997).

[11] I. Temizer, P. Wriggers, and T.J.R. Hughes *Contact Treatment in Isogeometric Analysis with NURBS.* Computer Methods in Applied Mechanics and Engineering, (2011), Vol. 200, pp. 1100–1112.

[12] T.E. Tezduyar, M. Behr, and J. Liou. *A new strategy for finite element computations involving moving boundaries and interaces - the deforming-spatial-domain/space-time procedure: I The concept and the preliminary numerical tests.* Computational Methods in Applied Mechanical Engineering,(1992), Vol. 94, pp. 339–351.

[13] T.E. Tezduyar, M. Behr, S. Mittal, and J. Liou. *A new strategy for finite element computations involving moving boundaries and interaces - the deforming-spatial-domain/space-time procedure: II Computations of free-surface flows, two-liquid flows, and flows with drifting cylinders.* Computational Methods in Applied Mechanical Engineering,(1992), Vol. 94, pp. 353–371.

[14] W.A. Wall. *Fluid-Struktur-Interaktionen mit stabilisierten Finiten Elementen.* Institut für Baustatistik der Universität Stuttgart, (1999).

[15] P. Wriggers, and T.A. Laursen. *Computational contact mechanics.* Vol.2, Springer,(2006).

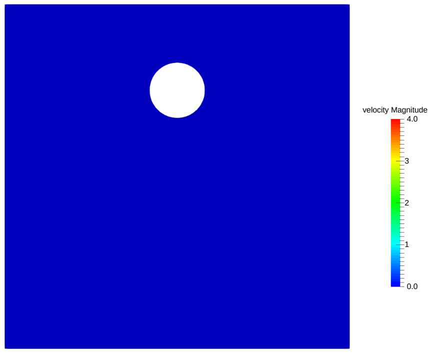

Figure 2: Velocity at $t = 0\,[\mathrm{s}]$.

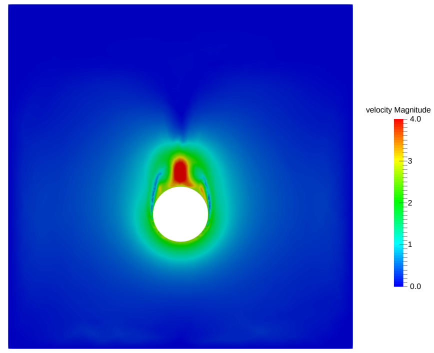

Figure 3: Velocity at $t = 0.55\,[\mathrm{s}]$.

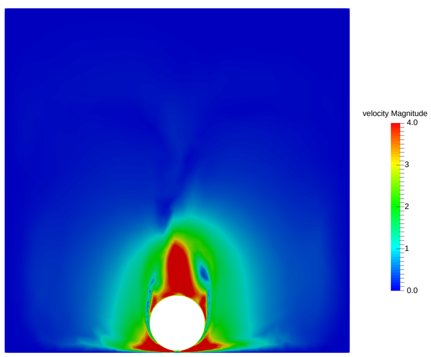

Figure 4: Velocity at $t = 0.75\,[\mathrm{s}]$.

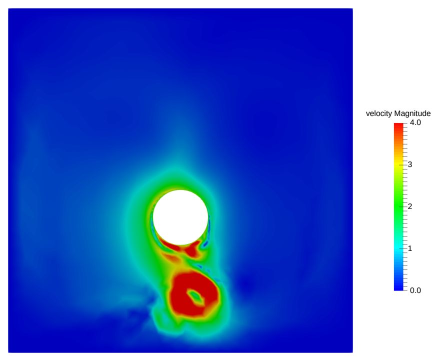

Figure 5: Velocity at $t = 1.0\,[\mathrm{s}]$.

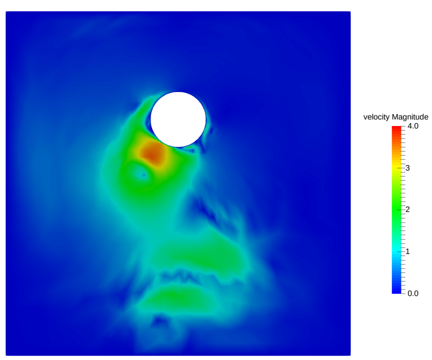

Figure 6: Velocity at $t = 1.45\,[\mathrm{s}]$.